be used to estimate $K_1$ from eq 11 at 3300 $M^{-1}$, although this value is, of course, subject to considerable uncertainty. An estimate for $K_2$ was not possible, since there was no indication of saturation at high [$Br^-$].

Conductometric and spectrophotometric determinations of ion-pair formation constants in DMF of some Cr(III) and Co(III) complexes with $Br^-$ show typical values near 800 for (1+, 1−) ion pairs[25-27] and 9200 for one example of a (2+, 1−) pair.[25] Our estimated value of 3300 for $K_1$ appears reasonable in this light. Data on ion triplet formation constants are sparse, but one determination for *cis*-$[Co(en)_2(DMF)Cl]^{2+}$ with $Cl^-$ in DMF resulted in a $K_2$ of 80.[25] With bromide ion we might expect smaller values.

The data in Table III indicate that $\phi_2 > \phi_3$, that is, the ion triplet is about three times more likely to yield the monobromo than the dibromo complex. If $K_2$ were estimated at 20 $M^{-1}$, $\phi_1$ and $\phi_3$ would be quite comparable, and $[Ru(bpy)_2(DMF)Br]^+$ would form more readily from the ion triplet than from the ion pair by about a factor of 3.

## Conclusion

In contrast with earlier studies using thiocyanate,[18] photoanation of $[Ru(bpy)_3]^{2+}$ by bromide ion in DMF can be fairly well accounted for by eq 11 and 12. These equations resulted from a model involving formation of both ion pairs and ion triplets as photoactive species. However, identical bromide dependences can be obtained from another model in which a monodentate bipyridine intermediate is formed from the ion pair as the single photochemical process, followed by thermal reactions (including further ion pairing of the intermediate) to form mono- and dianated species.[28]

We have interpreted our data in terms of the ion pair/ion triplet model because the derived formation constants appear reasonable and because no evidence for the monodentate intermediate has yet been found, even though a stable iridium(III) analogue has recently been reported.[29] It is in fact difficult to conceive of the dissociation of bipyridine proceeding other than through a monodentate intermediate (although not necessarily Ru(II)!), with which, however, both of the models presented here are consistent. It remains an interesting problem to differentiate between these closely related mechanisms.

A final point concerns the actual substitution mechanism. Although our treatment of the observable photoproducts (or even a model based on a monodentate–bipyridine intermediate) leads perhaps to the conclusion that classical ligand substitution is occurring, the rich redox chemistry of excited-state $[Ru(bpy)_3]^{2+}$ suggests also the possibility that the reaction proceeds through a Ru(III) or (in the presence of $Br^-$, for example) Ru(I) intermediate.

**Registry No.** $[Ru(bpy)_3]Br_2$, 15388-41-7; $Ru(bpy)_2Br_2$, 23377-85-7; $[Ru(bpy)_2(DMF)Br]^+$, 73663-67-9; $[Ru(bpy)_3]Cl_2$, 14323-06-9; $[Ru(bpy)_3]^{2+}$, 15158-62-0.

(25) I. R. Lantzke and D. W. Watts, *Aust. J. Chem.*, **19**, 969 (1966).
(26) W. A. Millen and D. W. Watts, *J. Am. Chem. Soc.*, **89**, 6858 (1967).
(27) D. A. Palmer and D. W. Watts, *Inorg. Chem.*, **10**, 281 (1971).
(28) The authors wish to thank Dr. Peter C. Ford for suggesting this mechanism.
(29) R. J. Watts, J. S. Harrington, and J. Van Houten, *J. Am. Chem. Soc.*, **99**, 2179 (1977).

Contribution from the Department of Chemistry, University of North Carolina, Chapel Hill, North Carolina 27514

# Rate of Electron Self-Exchange between the Delocalized Clusters $[Ru_3O(CH_3CO_2)_6(py)_3]^{+/0}$

JERRY L. WALSH, JOHN A. BAUMANN, and THOMAS J. MEYER*

*Received August 29, 1979*

Rate constants for electron self-exchange between the delocalized clusters $[Ru_3O(CH_3CO_2)_6(py)_3]^{+/0}$ at a series of temperatures were determined by analysis of line broadening observed for the acetate $^1H$ NMR resonances in solutions containing both clusters. At 24 °C, a rate constant of $1.1 \times 10^8$ $M^{-1}$ $s^{-1}$ was obtained for the self-exchange reaction, and kinetic parameters characterizing the reaction were determined from the temperature dependence of the rate constant: $\Delta H^*_{obsd}$(exptl) = 4.4 kcal/mol and $\Delta S^*_{obsd}$(exptl) = −7 cal/(mol deg). The results obtained from the self-exchange study are discussed in terms of a mechanism involving preassociation of the reactants, electron transfer within the association complex, and dissociation of the successor complex. The observed rate constant is then the product of a preequilibrium constant, $K_A$ (=exp($-\Delta G_A/RT$)), and the rate constant for electron transfer within the association complex, $k_{et}$ (=$\nu_{et}$ exp($-G^*/RT$)), $k_{obsd} = K_A k_{et}$. Theoretical calculations for the equilibrium constant and for the electron-transfer rate constant are presented and calculated kinetic parameters are compared to the experimental results. A statistical thermodynamic calculation of the preequilibrium constant results in a better agreement with the experimental results than that obtained by using the Eigen–Fuoss equation. Attempts to measure the rate of intramolecular electron transfer within the "mixed-valence" ligand-bridged dimer $[(py)_2Ru^{II}_3O(CH_3CO_2)_6(1,4\text{-pz})Ru^{0}_3O(CH_3CO_2)_6(py)_2]^+$ (1,4-pz is 1,4-pyrazine) using the NMR technique were unsuccessful but allowed an estimate of $k_{et} > 7 \times 10^4$ $s^{-1}$ at −70 °C to be made.

## Introduction

Recent experimental and theoretical advances have led to a more precise description of the microscopic events which occur during an electron-transfer process. In terms of theory, the earlier semiclassical treatments of Hush[1] and Marcus[2] have been reinforced and extended by more comprehensive quantum mechanical treatments.[3] One of the more important experimental advances has been based on the observation of intervalence transfer (IT) or metal–metal charge transfer (MMCT) absorption bands in specially designed mixed-va-

(1) (a) Hush, N. S. *Trans. Faraday Soc.* **1961**, *57*, 557; (b) *Prog. Inorg. Chem.* **1967**, *8*, 391; (c) *Electrochim. Acta* **1968**, *13*, 1005; (d) *Chem. Phys.* **1975**, *10*, 361.
(2) (a) Marcus, R. A.; Sutin, N. *Inorg. Chem.* **1975**, *14*, 213 and references therein. (b) Marcus, R. A. *J. Chem. Phys.* **1956**, *24*, 966; **1965**, *43*, 679.
(3) (a) Levich, V. G. *Adv. Electrochem. Electrochem. Eng.* **1966**, *4*, 249. (b) Dogonadze, R. R. "Reactions of Molecules at Electrodes"; Hush, N. S., Ed.; Wiley: New York, 1971. (c) Schmidt, P. P. *J. Electroanal. Chem.* **1977**, *82*, 29. (d) Kestner, N. R.; Logan, J.; Jortner, J. *J. Phys. Chem.* **1974**, *78*, 2148. (e) Christov, S. G. *Ber. Bunsenges. Phys. Chem.* **1975**, 79, 357. (f) Sondergaard, N. C.; Ulstrup, J.; Jortner, J. *Chem. Phys.* **1976**, *17*, 417. (g) Fischer, S. F.; Van Duyne, R. P. *Ibid.* **1977**, *26*, 9. (h) Efrima, S.; Bixon, M. *Ibid.* **1976**, *13*, 447.

0020-1669/80/1319-2145$01.00/0 

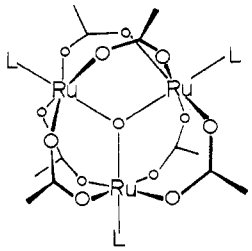

**Figure 1.** Structure of the cluster $[Ru_3O(CH_3CO_2)_6(L)_3]$.

lence dimers and oligomers[1,4] where electronic coupling is weak (e.g., eq 1; bpy is 2,2'-bipyridine). The value of the experiment

$$(bpy)_2ClRu^{II}N\bigcirc NRu^{III}Cl(bpy)_2^{3+} \xrightarrow{h\nu = E_{op}} (bpy)_2ClRu^{III}N\bigcirc NRu^{II}Cl(bpy)_2^{3+} \quad (1)$$

lies in the properties of the absorption bands since the work of Hush[1b-d] and more recently that of Hopfield[5] has shown that the band energy is directly related to the energy of activation for the related thermal process (eq 1–3), and it has

$$(bpy)_2ClRu^{II}N\bigcirc NRu^{III}Cl(bpy)_2^{3+} \xrightarrow{E_{th} = \Delta H^*} (bpy)_2ClRu^{III}N\bigcirc NRu^{II}Cl(bpy)_2^{3+} \quad (2)$$

$$E_{op} = 4E_{th} \quad (3)$$

been suggested that actual rate constants can be calculated by using both band energies and integrated intensities.[6]

Spencer and Wilkinson have reported the preparation of the trimeric, oxo-bridged cluster systems $[Ru_3O(CH_3CO_2)_6L_3]^{+/0}$ (L = neutral ligand)[7] (Figure 1), and we extended their work by showing that the clusters have an extensive, reversible electron-transfer chemistry, $[Ru_3O(CH_3CO_2)_6L_3]^{3+/2+/+/0/-/2-}$, and by examining the spectral properties of the 1+ and 0 clusters in some detail.[8,9] The results of the latter study suggest that the origin of the multiple electron-transfer character of the clusters is in a series of closely spaced molecular energy levels which are delocalized over the three metal sites.

The purpose of this paper is to present results that we have obtained on the electron-transfer reactivity of the cluster system, in particular the measurement of rate constants for the electron-transfer self-exchange reaction between $[Ru_3O(CH_3CO_2)_6(py)_3]^+$ (py is pyridine) and $[Ru_3O(CH_3CO_2)_6(py)_3]^0$, and to discuss our results in the context of electron-transfer theory. Our interests in the study were threefold. Although self-exchange rate constants are frequently available for single metal site based systems,[10] there are few if any cases where such measurements have been made for clusters. This is so even though the background redox chemistry has been documented for a number of systems,[11] and the experiment itself gives the most fundamental experimental insight into oxidation–reduction reactivity for a chemical system.

As a second point, we have developed a background synthetic chemistry which has led to the preparation of ligand-bridged cluster dimers,[9] like $[(py)_2(CH_3CO_2)_6Ru_3O(1,4\text{-}pz)Ru_3O(CH_3CO_2)_6(py)_2]^{2+}$, and also to higher oligomers. The ligand-bridged clusters have an extensive multiple electron-transfer chemistry, and one issue of interest is that the extent of electronic coupling between clusters appears to be a function of electron content.[9] In fact, there may be a transition from localized to delocalized behavior as the electron content of the clusters increases. For an understanding of the microscopic origins of such transitions, the important elements appear to be the extent of electronic coupling between sites and differences in inner- and outer-sphere vibrational structure which tend to localize excess electrons at a single redox site. The magnitude of the vibrational trapping energy can be estimated from self-exchange electron-transfer kinetic data.

Our third reason for interest was initially the most pressing. As mentioned earlier, theoretical treatments have been given which relate optical and thermal electron transfer[1,5] and the properties of IT absorption bands have been used to explore the role of medium and distance effects[4a,12] and to calculate rate constants for thermal electron transfer.[6] However, we have up to now been unsuccessful in devising a system where both the optical and thermal electron-transfer processes can be observed. For the mixed-valence dimer $[(py)_2(CH_3CO_2)_6Ru^I_3O(1,4\text{-}pz)Ru^0_3O(CH_3CO_2)_6(py)_2]^+$, a cluster-cluster IT band has been observed,[9] and it seemed possible that both measurements might be obtainable using the same

Table I. Compositions of the Solutions Used To Study the Self-Exchange Reaction of $[Ru_3O(CH_3CO_2)_6(py)_3]^{0/+}$ in Dichloromethane

| | sample | | | | | | | | |
|---|---|---|---|---|---|---|---|---|---|
| | A | B | C | D | E | F | G | H | I |
| $10^3C_T$,[a] M | 2.2 | 2.2 | 2.1 | 2.0 | 2.0 | 2.2 | 0.6 | 1.2 | 4.2 |
| $f_+$[b] | 0.00 | 1.00 | 0.15 | 0.38 | 0.52 | 0.82 | 0.32 | 0.34 | 0.31 |
| $f_0$[b] | 1.00 | 0.00 | 0.85 | 0.62 | 0.48 | 0.18 | 0.68 | 0.66 | 0.69 |

[a] Total concentration of 0 and 1+ clusters determined by the weight of added solid and the volume of solvent. [b] Mole fractions for the cationic ($f_+$) and neutral ($f_0$) clusters were determined from chemical shift data by assuming $\delta' = f_+\delta_+ + f_0\delta_0$.

Table II. Composition of Solutions Used To Study the Electron-Transfer-Exchange Reactions of the Ligand-Bridged Dimers $[(py)_2(CH_3CO_2)_6Ru_3O(L)Ru_3O(CH_3CO_2)_6(py)_2]^{n+}$ ($n$ = 0, 1, 2; L = Pyrazine, 4,4'-Bipyridine) in Dichloromethane

| | L = pyrazine[a] | | | | | | L = 4,4'-bipyridine[b] | |
|---|---|---|---|---|---|---|---|---|
| | 1[d] | 2 | 3 | 4 | 5 | 6 | 7 | 8 |
| $10^3C_T$,[c] M | 1.02 | 0.87 | 0.64 | 0.24 | 0.80 | 0.72 | 1.19 | 1.83 |
| $f_{2+}$ | 0.88 | 0.88 | 0.88 | 0.88 | 0.27 | 0.00 | 0.25 | 0.70 |
| $f_{1+}$ | 0.06 | 0.06 | 0.05 | 0.06 | 0.73 | 0.60 | 0.50 | 0.27 |
| $f_0$ | 0.06 | 0.06 | 0.07 | 0.06 | 0.00 | 0.40 | 0.25 | 0.03 |

[a] The fraction of each component ($f_{2+}$, $f_{1+}$, $f_0$) was calculated from equilibrium in eq 5 by using a value of $K = 250$. [b] The fraction of each component ($f_{2+}$, $f_{1+}$, $f_0$) was calculated from the equilibrium in eq 5 by using a value of $K = 4$. [c] Total concentration of 0, 1+, and 2+ dimers determined by the weight of added solid and the volume of solvent. [d] Sample numbers.

(4) (a) Tom, F. M.; Creutz, C.; Taube, H. *J. Am. Chem. Soc.* **1974**, *96*, 7827. (b) Callahan, R. W.; Keene, F. R.; Meyer, T. J.; Salmon, D. J. *Ibid.* **1977**, *99*, 1064. (c) Robin, M. B.; Day, P. *Adv. Inorg. Chem. Radiochem.* **1967**, *10*, 247. (d) Cowan, D. O.; LeVanda, C.; Park, J.; Kaufman, F. *Acc. Chem. Res.* **1973**, *6*, 1. (e) Meyer, T. J. *Ann. N.Y. Acad. Sci.* **1978**, *313*, 496.
(5) (a) Potasek, M. J.; Hopfield, J. J. *Proc. Natl. Acad. Sci. U.S.A.* **1977**, 229; (b) *Ibid.* **1977**, 3817.
(6) Meyer, T. J. *Chem. Phys. Lett.* **1979**, *64*, 417.
(7) (a) Spencer, A.; Wilkinson, G. *J. Chem. Soc., Dalton Trans.* **1972**, 1570. (b) Spencer, A.; Wilkinson, G. *Ibid.* **1974**, 786.
(8) Baumann, J. A.; Salmon, D. J.; Wilson, S. T.; Meyer, T. J.; Hatfield, W. E. *Inorg. Chem.* **1978**, *17*, 3342.
(9) (a) Baumann, J. A.; Wilson, S. T.; Salmon, D. J.; Hood, P. L.; Meyer, T. J. *J. Am. Chem. Soc.* **1979**, *101*, 2916. (b) Baumann, J. A.; Salmon, D. J.; Wilson, S. T.; Meyer, T. J. *Inorg. Chem.* **1979**, *18*, 2472.
(10) Sykes, A. G. *Adv. Inorg. Chem. Radiochem.* **1976**, *10*, 153. Sutin, N. *Inorg. Biochem.* **1973**, *2*, 611.
(11) Meyer, T. J. *Prog. Inorg. Chem.* **1975**, *19*, 1.
(12) Meyer, T. J. *Acc. Chem. Res.* **1978**, *11*, 94; Powers, M. J.; Meyer, T. J. *J. Am. Chem. Soc.* **1980**, *102*, 1289; and references therein.
(13) Yang, E. S.; Chan, M.-S.; Wahl, A. C. *J. Phys. Chem.* **1975**, *79*, 2049.
(14) Pople, J. A.; Schneider, W. G.; Bernstein, H. J. "High-Resolution Nuclear Magnetic Resonance"; McGraw-Hill: New York, 1959.

NMR technique that was successful for the electron transfer self-exchange reaction.

## Experimental Section

The compounds used in the kinetic studies were prepared as previously described.[8,9] Dichloromethane-$d_2$ was obtained from Merck and used without further purification. Kinetic samples were prepared by weighing the appropriate quantities of solid reagents into 5-mm Pyrex NMR tubes, adding a known volume of solvent, freeze–thaw degassing, and sealing under vacuum. Samples were stored at −80 °C. Total cluster concentration was calculated from the weight of solid and volume of solvent added to the NMR tube. For the monomer mixtures, the mole fraction of each component was obtained from chemical shift data, by assuming $\delta' = f_0\delta_0 + f_+\delta_+$ where $\delta'$, $\delta_0$, and $\delta_+$ are the chemical shifts of the acetate protons observed for solutions containing the sample mixture and pure 0 and pure 1+ clusters, respectively, and $f_0$ and $f_+$ are the mole fractions of 0 and 1+, respectively, in the sample mixture. Samples of the ligand-bridged dimers, $[(py)_2(CH_3CO_2)_6Ru_3O(L)Ru_3O(CH_3CO_2)_6(py)_2]^{n+}$ ($n$ = 0, 1, 2) (L = pyrazine, 4,4′-bipyridine), were prepared by the same route as the monomeric samples. The mixed-valence dimers ($n$ = 1+) were prepared both from isolated bulk samples of the mixed-valence species and by mixing equimolar quantities of the $n$ = 0 and $n$ = 2 components. The compositions of the monomeric samples and the ligand-bridged dimers used for the kinetic studies are listed in Tables I and II, respectively. For the most part, spectra were obtained at about 15° intervals between +24 and −90 °C.

Spectra were obtained on a Varian XL-100 spectrometer equipped with a variable-temperature controller. Probe temperatures were measured with a low-temperature thermometer which was calibrated by using methanol chemical shift data. Chemical shifts were determined relative to tetramethylsilane as an internal standard.

Second-order rate constants, $k$, for outer-sphere self-exchange between $[Ru_3O(CH_3CO_2)_6(py)_3]^0$ and $[Ru_3O(CH_3CO_2)_6(py)_3]^+$ were determined by interpreting the line broadening observed for the acetate $^1H$ resonances in terms of a two-site-exchange model with exchange occurring between a diamagnetic and paramagnetic site.

The observed line widths were analyzed by using eq 4 where $W'$,

$$W' = f_0W_0 + f_+W_+ + [f_0f_+(4\pi)(\Delta\nu)^2/kC_T] \quad (4)$$

$W_0$, and $W_+$ are line widths at half-height for solutions containing the sample mixture and pure 0 and pure 1+ clusters, respectively, $\Delta\nu$ is the separation in Hz of the $^1H$ resonances of the acetate groups for the 0 and 1+ clusters, and $C_T$ is the total concentration of 0 and 1+ clusters. Equation 4 was derived from the Bloch equations for a two-site exchange system under the conditions that (1) the transverse relaxation time for the 0 and 1+ components are not equal, (2) the rate law is first order in each component, and (3) $2\pi\tau(\Delta\nu) \ll 1$ where $\tau$ is the chemical-exchange lifetime.

## Results

In solutions containing either the 0 or 1+ clusters, $[Ru_3O(CH_3CO_2)_6(py)_3]^{+/0}$, resonances for all the protons are observed as shown in Figure 2A,B. A singlet is observed for the acetate protons, and three resonances of varying complexity are observed for the ortho, meta, and para protons of the pyridyl groups. For the paramagnetic 1+ clusters, the resonances are shifted considerably compared to the 0 clusters and the shifts are strongly temperature dependent. As the temperature is lowered, the resonances for the acetate protons move downfield compared to the room-temperature position (see Figure 2C). For the pyridyl protons, the resonances move upfield and the relative magnitude of the shifts are ortho > meta > para.

Samples containing mixtures of the 0 and 1+ clusters also show only one set of proton resonances at room temperature (Figure 3); chemical shift data are available as supplementary material. On the basis of the compositions of the solutions, the positions of the signals are found where they might be expected if there were a complete averaging of the 0 and 1+ resonances. At room temperature, the resonances are relatively sharp, but as the temperature is lowered the signals broaden noticeably (Figure 3). The extent of broadening is significantly greater than the temperature-induced broadening observed in solutions containing only pure 1+ or 0 clusters.

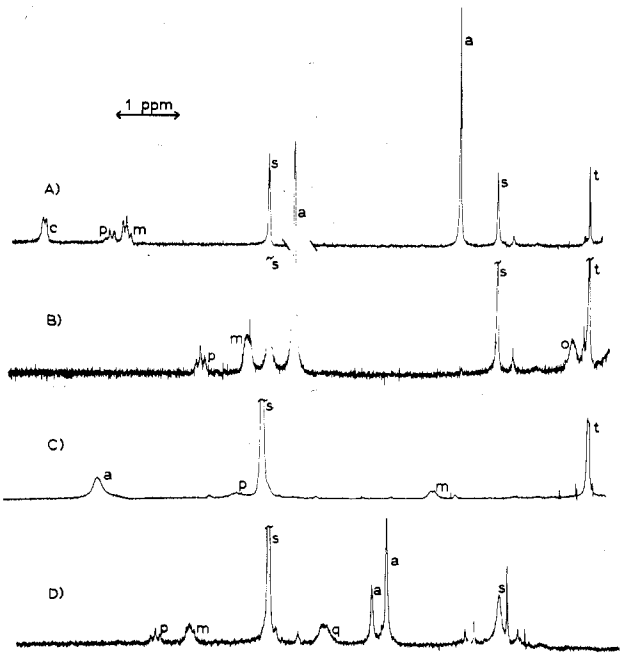


**Figure 2.** (A) $^1H$ NMR spectrum of $[Ru_3O(CH_3CO_2)_6(py)_3]$ in $CD_2Cl_2$ at 24 °C. (B) $^1H$ NMR spectrum of $[Ru_3O(CH_3CO_2)_6(py)_3]^+$ in $CD_2Cl_2$ at 24 °C. (C) Same as B, −80 °C. (D) $^1H$ NMR spectrum of $[(py)_2(CH_3CO_2)_6Ru_3O(1,4\text{-}py)Ru_3O(CH_3CO_2)_6(py)_2]^+$ in $CD_2Cl_2$ at 24 °C. (Small quantities of the 0 and 2+ dimers are also present according to eq 5.) Labels: a = acetate, t = $Me_4Si$, s = solvent, o = *o*-pyridine, m = *m*-pyridine, p = *p*-pyridine, q = pyrazine.

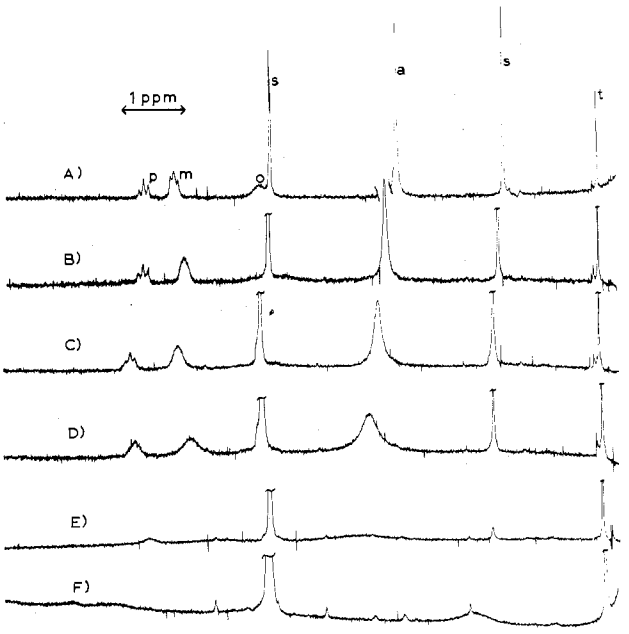


**Figure 3.** Temperature dependence of the $^1H$ NMR spectrum of a mixture of $[Ru_3O(CH_3CO_2)_6(py)_3]^{+/0}$ in $CD_2Cl_2$ ($C_T$ = 2.0 mM; $f_+$ = 0.38, $f_0$ = 0.62): (A) 24 °C, (B) −10 °C, (C) −30 °C, (D) −47 °C, (E) −66 °C, (F) −92 °C. Labels: a = acetate, t = $Me_4Si$, s = solvent, o = *o*-pyridine, m = *m*-pyridine, p = *p*-pyridine.

The enhanced broadening can be attributed to the exchange process in which electron transfer occurs between the 1+ and 0 clusters. At the lowest temperature at which spectra were obtained (−92 °C), separate acetate resonances are observed for the 1+ and 0 clusters (Figure 3F), showing that the slow-exchange limit had been reached.

Rate constants, calculated from the line-broadening data using eq 4, are given in Table III. Experimentally, the ability

**Table III.** Rate Constants for the Self-Exchange Reaction of $[Ru_3O(CH_3CO_2)_6(py)_3]^{+/0}$ in Dichloromethane

| | $10^{-7}k$, $M^{-1}$ $s^{-1}$ [a] | | | | | | | |
|---|---|---|---|---|---|---|---|---|
| $T$, °C | C | D | E | F | G | H | I | av (av dev) |
| 33 | | | | | 12.4 | | | 12.4 |
| 24 | 11.4 | 11.0 | 12.0 | 12.7 | 9.2 | 12.6 | | 11.5 (1.0) |
| 7 | 11.5 | 4.6 | 14.6 | 7.7 | 5.4 | 5.9 | 5.3 | 7.6 (1.8) |
| −10 | 4.0 | 4.9 | 5.8 | 4.0 | 2.9 | 3.7 | 4.4 | 4.7 (0.8) |
| −30 | 2.1 | 1.9 | 2.2 | 1.1 | | 2.2 | 1.8 | 2.0 (0.4) |
| −47 | 1.4 | 1.3 | 1.2 | 0.4 | | 1.1 | 0.8 | 0.9 (0.3) |
| −66 | 0.4 | 0.4 | 0.5 | 0.6 | | | 0.4 | 0.5 (0.1) |

[a] The letters below refer to the solution compositions defined in Table I.

to adjust total and relative concentrations of the clusters and the second-order nature of the process allowed adjustment of the lifetime, and, hence, the line-broadening effects can be analyzed over a considerable range of temperatures. Some of the data presented in Table III are marginally acceptable on the basis of the criteria set by Gutowsky et al.,[15] but they have been included since they are statistically consistent with the bulk of the data.

An attempt was made to observe line-broadening processes and hopefully to measure rate constants for intramolecular electron transfer in the ligand-bridged dimers $[(py)_2(CH_3CO_2)_6Ru^{I}_3O(1,4\text{-pz})Ru^{0}_3O(CH_3CO_2)_6(py)_2]^+$ and $[(py)_2(CH_3CO_2)_6Ru^{I}_3O(4,4'\text{-bpy})Ru^{0}_3O(CH_3CO_2)_6(py)_2]^+$ (4,4′-bpy is 4,4′-bipyridine). Before discussing the analysis, it is important to realize that there are competitive outer-sphere reactions which can also lead to electron exchange.

In solutions containing the mixed-valence dimers, denoted by [0,1], there are always at least small amounts of the [0,0] and [1,1] dimers because of the comproportionation equilibrium in eq 5. Values of $K$ for the equilibrium can be calcu-

$$[0,0] + [1,1] \overset{K}{\rightleftharpoons} 2[0,1] \quad (5)$$

lated from electrochemical data.[9a] Under the conditions of the NMR experiment, $K = 250$ and $\geq 4$ for the pyrazine- and 4,4′-bipyridine-bridged dimers, respectively.

Because of the equilibrium in eq 5, bimolecular pathways for exchange involving outer-sphere electron transfer (eq 6–8)

$$[0,1] + [0,0] \rightleftarrows [0,0] + [0,1] \quad (6)$$

$$[0,1] + [1,1] \rightleftarrows [1,1] + [0,1] \quad (7)$$

$$2[0,1] \rightleftarrows [1,1] + [0,0] \rightleftarrows 2[1,0] \quad (8)$$

are present in addition to the intramolecular electron-exchange process which is the reaction of primary interest (eq 9). The

$$[0,1] \rightleftarrows [1,0] \quad (9)$$

values of $K$ for the two dimers show that for the pyrazine-bridged case only small amounts of [0,0] and [1,1] are present in solutions of [0,1] at equilibrium, but for the 4,4′-bipyridine-bridged case, relatively more significant quantities of the [0,0] and [1,1] species are present. For this reason, interferences from the two outer-sphere reactions in eq 6 and 7 should be relatively minor for the pyrazine-bridged dimer in that the processes should be far slower than intramolecular electron transfer. For the 4,4′-bipyridine-bridged dimer, the reactions in eq 6 and 7 will be of more importance because higher concentrations of the 0 and 2+ dimers are present. The bimolecular reaction in eq 8 is equivalent to eq 9 in the net sense but is second rather than first order. Unless intramolecular electron transfer is inhibited, eq 9 will always be more rapid than eq 8 because the vibrational barriers to electron transfer will at least be about the same, and in the outer-sphere case, an initial step in which the electron-donor and -acceptor sites are brought together must precede the electron-transfer step.

Room-temperature NMR spectra of solutions containing only the 0 or 2+ clusters, [0,0] or [1,1], with either bridging ligand include two acetate $^1H$ resonances in a 2:1 ratio. This pattern is expected since the acetate groups are magnetically nonequivalent with four of the acetate groups adjacent and two opposite the bridging ligand (note Figure 1). Some but not all of the expected pyridine, pyrazine, and 4,4′-bipyridine $^1H$ resonances are observed. As in the monomer spectra, the proton resonances of the [1,1] clusters, which are paramagnetic, are shifted appreciably from the positions for the diamagnetic clusters and their positions are strongly temperature dependent. Solutions containing mixtures of the [0,0], [0,1], and [1,1] dimers also exhibit only one set of acetate $^1H$ resonances at room temperature (Figure 2D), indicating that electron transfer is rapid between all of the cluster sites under these conditions. The positions observed for the signals can be accounted for if complete electron-transfer averaging occurs for all of the components added to the solutions and if it is assumed that the position of the resonances for the pure [0,1] dimer is an average of those for the [0,0] and [1,1] dimers.

For solutions containing mixtures of the pyrazine-bridged dimers, [0,0], [0,1], and [1,1], the acetate $^1H$ resonances broaden as the temperature is lowered below room temperature. Typically at about −30 °C, only a very broad resonance is observed. Below this temperature two sets of acetate resonances appear for solutions containing relatively large amounts of both the [0,1] and [1,1] dimers. One set was located at the position of pure [1,1] and the others, independent of relative concentration, at a position midway between the [1,1] and [0,0] resonances. These results indicate that under the conditions of the experiment, outer-sphere electron transfer, which is dominated by eq 6 and 7, has been slowed to the slow-exchange limit. The observed signals are attributable to the [1,1] and [0,1] dimers, and for the mixed-valence dimer, [0,1], inner-sphere electron transfer is still rapid at −30 °C. With −30 °C as an approximate coalescence temperature, the lifetime for outer-sphere electron exchange via eq 6–8 is ~1 ms under the conditions of the experiment.[14] Because of the complexity of the exchange processes, no attempt was made to calculate rate constants but estimates are in the range observed for the monomer self-exchange which is reasonable given the nature of the reaction.

The experiment with added [1,1] dimer shows that outer-sphere processes can be frozen out at temperatures where inner-sphere exchange is still rapid. Unfortunately, at the lowest temperature at which measurements were possible, there is no sign of line broadening for the exchange averaged [1,0] resonance. From this result a lower limit for the rate constant for the intramolecular electron-exchange reaction in eq 9 at −70 °C is calculated to be $k > 7 \times 10^4$ $s^{-1}$.

At this point an experiment to determine the temperature dependence of the $^1H$ NMR spectrum for the 4,4′-bipyridine-bridged dimer, [0,1], was attempted. Earlier work[16] with mixed-valence complexes has shown that both the energy of the IT transition and, by inference, the thermal activation energy (eq 3) increase as the distance separating the redox sites increases because of a medium polarization effect. Because of the greater intercluster separation where 4,4′-bipyridine is the bridge compared to pyrazine (11.1 vs. 6.9 Å),[16] the rate constant for intramolecular electron transfer should be slower for the 4,4′-bpy dimer. The room-temperature spectra obtained for the 4,4′-bpy dimer were qualitatively similar to those obtained for similarly constituted solutions

(15) Allerhand, A.; Gutowsky, H. S.; Jonas, J.; Meinzer, R. A. *J. Am. Chem. Soc.* **1966**, *88*, 3185.

(16) Callahan, R. W.; Meyer, T. J.; Powers, M. J.; Salmon, D. J. *J. Am. Chem. Soc.* **1976**, *98*, 6731.

Table IV. Kinetic Parameters for the Self-Exchange Reaction of $[Ru_3O(CH_3CO_2)_6(py)_3]^{+/0}$ in Dichloromethane[a]

| parameter | exptl value |
|---|---|
| $\Delta H^*_{obsd} = \Delta H_A + \Delta H^*$ | 4.4 kcal/mol |
| $\Delta S^*_{obsd} + R \ln \nu_{et}$[a] | 52 cal/(mol deg) |

[a] Note eq 15 and 16. [b] $\Delta S^*_{obsd} = \Delta S_A + \Delta S^*$.

containing the pyrazine-bridged dimer. However, these solutions, either with or without the corresponding [0,0] or [1,1] dimers added, exhibited no exchange broadening down to −70 °C. Apparently, the sizable concentrations of the [0,0] and [1,1] dimers, which exist because of the comproportionation equilibrium in eq 5, result in enhanced outer-sphere electron-transfer rates, and their measurement by line broadening is inaccessible in the temperature range available. Obviously, no information concerning intramolecular electron transfer could be obtained from the experiments.

## Discussion

The relative magnetic properties of the clusters, $[Ru_3O(CH_3CO_2)_6(py)_3]^{+/0}$, provide a particularly convenient means with which to study electron self-exchange by NMR. The line widths are narrow in both cases, the paramagnetic isotropic shifts for the 1+ clusters are appreciable but not excessive, and the acetate resonance is a convenient singlet. Although the 1+ monomer and the 1+ and 2+ dimers are paramagnetic, there appear to be little or no paramagnetic contributions to the widths of the NMR resonances. This phenomenon has been discussed in terms of a very rapid electron-spin relaxation for $S = {}^1/_2$ systems which have either degenerate ground states or low-lying excited states.[17,18] With the present data, the magnitude of the dipolar and contact contributions to the isotropic shifts can not be established. Although the direction of the isotropic shift for the acetate protons is opposite that of the pyridyl protons, the effect could be due to different spatial orientations if dipolar contributions are the dominant feature or to hyperfine coupling constants with different signs if contact contributions are important. The magnetic character of the dimers appears to be the sum of the characters of the component monomers.

The outer-sphere self-exchange reaction between the 0 and 1+ clusters, $[Ru_3O(CH_3CO_2)_6(py)_3]^{+/0}$, gives further insight into the redox properties of the clusters and provides a basis for beginning to understand the properties of the dimers and higher oligomers referred to in the Introduction.[9] The data also provide one of the few examples where quantitative information about a cluster-based electron-transfer process is available and are of value in the context of a discussion based on electron-transfer theory.

The rate constant for self-exchange of $1.1 \times 10^8$ $M^{-1}$ $s^{-1}$ at 24 °C for the 0 and 1+ monomers is comparable to the most rapid rate constants reported for self-exchange reactions on the basis of single metal redox site systems.[10] However, the value is considerably below the calculated diffusion-controlled limit[19] ($k_D = 1.5 \times 10^{10}$ $M^{-1}$ $s^{-1}$), and there is apparently a finite vibrational trapping barrier which inhibits electron transfer between the clusters.

Our treatment and interpretation of the kinetic data will be based on the scheme below where in the first step the two reacting clusters diffuse together to form an association complex (eq 10) followed by electron transfer within the association complex (eq 11) and the breakup of the successor complex (eq 12).

$$Ru^I_3O(CH_3CO_2)_6(py)_3^+ + Ru^0_3O(CH_3CO_2)_6(py)_3 \overset{K_A}{\rightleftharpoons} [Ru^I_3O(CH_3CO_2)_6(py)_3,Ru^0_3O(CH_3CO_2)_6(py)_3]^+ \quad (10)$$

$$[Ru^I_3O(CH_3CO_2)_6(py)_3,Ru^0_3O(CH_3CO_2)_6(py)_3] \xrightarrow{k_{et}} [Ru^0_3O(CH_3CO_2)_6(py)_3,Ru^I_3O(CH_3CO_2)_6(py)_3]^+ \quad (11)$$

$$[Ru^0_3O(CH_3CO_2)_6(py)_3,Ru^I_3O(CH_3CO_2)_6(py)_3]^+ \rightarrow Ru^0_3O(CH_3CO_2)_6(py)_3 + Ru^I_3O(CH_3CO_2)_6(py)_3^+ \quad (12)$$

The experimentally observed rate constants, $k$, are sufficiently slow that it is not necessary to make corrections for diffusional effects.[19] It follows, from the scheme in eq 10–12, that for the thermally activated electron-transfer process

$$k = K_A k_{et} \quad (13)$$

Based on the scheme in eq 10–12 and using eq 13, it is possible to interpret the rate-constant data, including its temperature dependence. For the electron-transfer step, $k_{et}$ can be written as the product of a frequency factor term ($\nu_{et}$) and an exponential term whose origin lies in vibrational trapping of the excess electron on one of the clusters (eq 14). In eq

$$k_{et} = \nu_{et} \exp(-\Delta G^*/RT) = \nu_{et} \exp(-\Delta H^*/RT) \exp(\Delta S^*/R) \quad (14)$$

14, $\Delta H^*$ is a measure of the extent of thermal activation or the depth of the trapping well, $\Delta S^*$ is a measure of changes in the density of states of the critical vibrational modes involved in the activation process, and $\Delta G^* = \Delta H^* - T\Delta S^*$. Associated with the preequilibrium step in eq 10 is an equilibrium constant, $K_A$, which is related to the associated thermodynamic quantities, $\Delta G_A$, $\Delta H_A$, and $\Delta S_A$, as shown in eq 15. Com-

$$K_A = \exp(-\Delta G_A/RT) = \exp(-\Delta H_A/RT) \exp(\Delta S_A/R) \quad (15)$$

bining eq 14 and 15 according to eq 13 gives eq 16 which is

$$k = \nu_{et}K_A \exp(-\Delta G^*/RT) = \nu_{et} \exp[(\Delta S^* + \Delta S_A)/R] \exp[-(\Delta H^* + \Delta H_A)/RT] = \nu_{et} \exp(\Delta S^*_{obsd}/R) \exp(-\Delta H^*_{obsd}/RT) \quad (16)$$

an expression relating the experimentally observed rate constant to its two component steps including their temperature dependences.

In terms of the activation parameters of the more usually encountered, but microscopically less appropriate, reaction rate theory expression (eq 17), the terms developed above are given

$$k = (k_bT/h) \exp(-\Delta G^{\ddagger}/RT) = (k_bT/h) \exp(-\Delta H^{\ddagger}/RT) \exp(\Delta S^{\ddagger}/R) \quad (17)$$

in eq 18–20. In these equations, $k_b$ is Boltzmann's constant

$$\Delta H^{\ddagger} = \Delta H_A + \Delta H^* - RT = \Delta H^*_{obsd} - RT \quad (18)$$

$$\Delta S^{\ddagger} = \Delta S_A + \Delta S^* + R \ln (\nu_{et}h/k_bT) - R = \Delta S^*_{obsd} + R \ln (\nu_{et}h/k_bT) - R \quad (19)$$

$$\Delta G^{\ddagger} = \Delta G_A + \Delta G^* + RT \ln (k_bT/h\nu_{et}) = \Delta G^*_{obsd} + RT \ln (k_bT/h\nu_{et}) \quad (20)$$

and $h$ is Planck's constant. Conceptually, eq 16 is more valuable than eq 17 since it is based on a microscopically precise model for the process of interest. It should also be noted that a comparison between the two is not arbitrary since in related systems it appears that the individual terms $\nu_{et}$, $K_A$, and $\exp(-\Delta H^*/RT)$ can be evaluated experimentally.

From eq 16, with the assumption that the temperature dependence of $\nu_{et}$ is sufficiently small that it can be treated as a constant, a plot of ln $k$ vs. $T^{-1}$ is predicted to give as slope $-(\Delta H^* + \Delta H_A)/R$ and as intercept $(\Delta S^* + \Delta S_A)/R + \ln \nu_{et}$. In Figure 4 is shown a plot of ln $k$ vs. $T^{-1}$, and in Table IV

(17) Swift, T. S. "NMR of Paramagnetic Molecules, Principles and Applications"; Academic Press: New York, 1973.
(18) Doddrell, D. M.; Pegg, D. T.; Bendall, M. R.; Gregson, A. K. *Aust. J. Chem.* **1978**, *31*, 2355 and references therein.
(19) Noyes, R. M. *Prog. React. Kinet.* **1961**, *1*, 129.

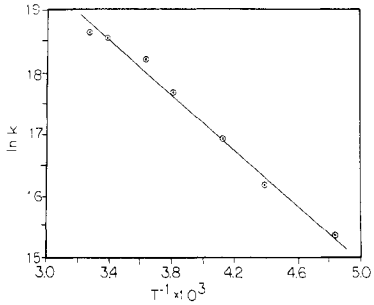


**Figure 4.** Plot of $k$ vs. $1/T$ for the temperature dependence of the self-exchange rate constants for the clusters $[Ru_3O(CH_3CO_2)_6(py)_3]^{+/0}$.

are given the numerical values for the terms $\Delta H^*_{obsd} = \Delta H^* + \Delta H_A$ and $\Delta S^*_{obsd} + R \ln \nu_{et} = \Delta S^* + \Delta S_A + R \ln \nu_{et}$. The values were calculated from the best values of the slope and intercept of the plot determined by a linear least-squares analysis of the data.

Our interest in the experimentally derived values for the enthalpic and entropic terms is for purposes of comparison with values calculated from available theoretical equations.[1,2] For the preequilibrium involving formation of the association complex, the equilibrium constant $K_A$ can be calculated by using the Eigen–Fuoss equation (eq 21),[20] in which $d$ is the center to center contact distance and $N$ is Avogadro's number, or from eq 22 which is derived from a statistical thermodynamic treatment[21] and which has been discussed in the context of the electron-transfer problem by Marcus et al.[22] and by Brown and Sutin.[23] In eq 22, $\mu$ is the reduced mass of the reactants A and B ($\mu = M_A M_B/(M_A + M_B)$), $V$ is the molar volume (molecular weight/density) of the solvent, and $V_f = V - V_W$ where $V_W$ is the van der Waals or "free volume" of the solvent.[24] Since $\Delta G_A = -RT \ln K_A$, $\Delta H_A = \partial(\Delta G/T)/\partial(1/T)$, and $\Delta S_A = -\partial \Delta G/\partial T$, it follows that from the Eigen–Fuoss equation

$$K_A = 4\pi N d^3/3000 \tag{21}$$

$$K_A = (V/V_f)d^2(8\pi h^2/\mu k_B T)^{1/2}(N/1000) \tag{22}$$

$$\Delta G_A = -RT \ln (4\pi N d^3/3000) \tag{23}$$

$$\Delta H_A = 0 \tag{24}$$

$$\Delta S_A = R \ln (4\pi N d^3/3000) \tag{25}$$

and from the statistical equation

$$\Delta G_A = -RT \ln [(V/V_f)d^2(8\pi h^2/\mu k_B T)^{1/2}(N/1000)] \tag{26}$$

$$\Delta H_A = -RT/2 \tag{27}$$

$$\Delta S_A = R \ln [(V/V_f)d^2(8\pi h^2/\mu k_B T)^{1/2}(N/1000)] - R/2 \tag{28}$$

In terms of gross structure, the clusters are nonspherical and estimates of the minimum (along the axis perpendicular to the $Ru_3O$ plane) and maximum (along the central O–Ru–pyridine axes) molecular radii including van der Waals volumes on the periphery are 5.8 and 9.0 Å.[25] Using as an approximation an average molecular radius of 7 Å gives for the close contact distance in the association complex $d = 14$ Å. With that value of $d$ and $V/V_f = 2.1$ for dichloromethane,[24] values can be calculated for $K_A$, $\Delta G_A$, $\Delta H_A$, and $\Delta S_A$. The results obtained by using the two different models (eq 21–28) are shown here

| | Eigen–Fuoss | statistical |
|---|---|---|
| $K_A$, $M^{-1}$ | 6.9 | 0.14 |
| $\Delta G_A$, kcal/mol | −1.1 | 1.2 |
| $\Delta H_A$, kcal/mol | 0 | −0.3 |
| $\Delta S_A$, cal/(mol deg) | 2.8 | −4.9 |

and it is clear that they make rather different predictions about the quantitative details of the preassociation step.

For the outer-sphere electron-transfer step within the association complex (eq 11), a vibrational trapping barrier exists to the transfer of the excess electron. The origin of the barrier, which is given by eq 29,[1,2] lies in the differences in inner- ($\lambda_i$)

$$\Delta G^* = \lambda_i/4 + \lambda_o/4 \tag{29}$$

and outer-sphere ($\lambda_o$) vibrational structures at the two cluster sites.[1,2] A proper treatment of $\lambda_i$ requires a detailed vibrational analysis of the individual clusters and a recognition of the quantum mechanical nature of the problem. However, the low-energy infrared spectra of the 1+ and 0 clusters are relatively similar, suggesting that differences in the skeletal structures are slight and that $\lambda_i$ may be small.[8] The implied absence of a significant structural difference is certainly consistent with the delocalized nature of the cluster redox levels.

With use of a dielectric continuum treatment for the solvent, $\lambda_o$ is given by eq 30, where $e$ is the unit electric charge, $a_1$ and

$$\lambda_o = e^2\left(\frac{1}{2a_1} + \frac{1}{2a_2} - \frac{1}{d}\right)\left(\frac{1}{D_{op}} - \frac{1}{D_s}\right) \tag{30}$$

$a_2$ are the van der Waals radii of the reactants, $D_{op}$ is the optical dielectric constant, and $D_s$ is the static dielectric constant.[1,2] For the self-exchange reaction studied here, $a_1 \approx a_2 \approx d/2$, so that eq 30 can be simplified to give eq 31. With

$$\lambda_o = \frac{e^2}{2a}\left(\frac{1}{D_{op}} - \frac{1}{D_s}\right) \tag{31}$$

the assumption that $\lambda_i \approx 0$ and by use of the fact that $D_{op}$ is relatively independent of temperature, the following set of equations can be derived[22,23] ($\theta = -\partial \ln D_s/\partial \ln T$).

$$\Delta G^* = \frac{\lambda_o}{4} = \frac{e^2}{8a}\left(\frac{1}{D_{op}} - \frac{1}{D_s}\right) \tag{32}$$

**Table V.** Comparison between Experimental and Calculated Kinetic Parameters ($H$ in kcal/mol; $S$ in cal/(mol deg))[a]

| $\Delta H_A$ | $\Delta H^*$ | $\Delta H^*_{obsd} = \Delta H_A + \Delta H^*$ | $\Delta H^*_{obsd}$ (exptl) |
|---|---|---|---|
| 0 (eq 24) | 3.5 (eq 33) | 3.5 | 4.4 |
| −0.3 (eq 27) | 3.5 (eq 33) | 3.2 | 4.4 |
| $\Delta S_A$ | $\Delta S^*$ | $\Delta S^*_{obsd} = \Delta S_A + \Delta S^*$ | $\Delta S^*_{obsd}$ (exptl)[b] |
| 3.8 (eq 25) | 2.6 (eq 34) | +6 | −7 ± 5 |
| −4.9 (eq 28) | 2.6 (eq 34) | −2 | −7 ± 5 |

[a] The equations used to obtain the calculated values are given in parentheses. [b] Assuming that $\nu_{et} = 10^{13}$; note Table IV and recall that $\Delta S^*_{obsd} - R \ln \nu_{et} = \Delta S^* + \Delta S_A + R \ln \nu_{et} = 52$ cal/(mol deg).

(20) (a) Fuoss, R. M. *J. Am. Chem. Soc.* **1958**, *80*, 5059. (b) Petrucci, S. In "Ionic Interactions"; Petrucci, S., Ed.; Academic Press: New York, 1971; Vols. I and II. (c) Eigen, M.; Kruse, W.; Maass, G.; Maeyer, D. L. *Prog. React. Kinet.* **1964**, *2*, 287.
(21) North, A. M. "The Collision Theory of Chemical Reactions in Liquids"; Wiley: New York, 1964.
(22) Waisman, E.; Worry, G.; Marcus, R. A. *J. Electroanal. Chem.* **1977**, *82*, 9.
(23) Brown, G. M.; Sutin, N. *J. Am. Chem. Soc.* **1979**, *101*, 883.
(24) Edward, J. T. *J. Chem. Educ.* **1978**, *47*, 261.
(25) Distances were estimated by using the structural data for $Ru_3O(CH_3CO_2)_6(PPh_3)_3$[26a] and a Ru–pyridine radius of 7.1 Å.[26b]
(26) (a) Cotton, F. A.; Norman, J. G. *Inorg. Chim. Acta* **1972**, *6*, 411. (b) Powers, M. J. Ph.D. Thesis, University of North Carolina, Chapel Hill, NC, 1977.

$$\Delta H^* = \frac{\partial(\Delta G^*/T)}{\partial(1/T)} = \frac{\lambda_o}{4} + \frac{e^2\theta}{8aD_s} \quad (33)$$

$$\Delta S^* = \frac{-\partial \Delta G^*}{\partial T} = \frac{e^2\theta}{8aD_sT} \quad (34)$$

We are now in a position to make comparisons between calculated and experimental kinetic parameters. The data are collected in Table V where, for the calculated values, the equations used in the calculations are given in parentheses. For the $[Ru_3O(CH_3CO_2)_6(py)_3]^{+/0}$ self-exchange reaction in methylene chloride[27] at 24 °C, the calculated values of $\Delta G^*$, $\Delta H^*$, and $\Delta S^*$ using eq 32–34 are 2.7 kcal/mol, 3.5 kcal/mol, and 2.6 cal/(mol deg), respectively. For the overall enthalpic term, $\Delta H_A + \Delta H^*$, the agreement between the experimental (4.5 kcal/mol) and calculated (3.5 or 3.2 kcal/mol) values using either the Eigen–Fuoss or statistical approaches is reasonable and tends to reinforce the conclusion that the primary origin of the vibrational trapping barrier is in the medium surrounding the clusters.[1,2]

From the intercept of the plot of Figure 4, the experimental value of $\Delta S_A + \Delta S^* + R \ln \nu_{et}$ is 52 cal/(mol deg). Before any comparisons can be made between calculated and experimental values of the sum $\Delta S_A + \Delta S^*$, a value must be estimated for $\nu_{et}$, the frequency factor for electron transfer. A reasonable estimate for $\nu_{et}$ is $10^{13} \pm 10$ $s^{-1}$. The estimate comes from recent results based on the observation of metal–metal charge transfer (MMCT) or intervalence transfer (IT) transitions in outer-sphere complexes like $[Ru^{III}(NH_3)_5py,Fe^{II}(CN)_6]^-$.[28] From an analysis of the MMCT absorption band, it has been concluded[28] that electronic coupling between the donor and acceptor sites is comparable to that between Ru(II) and Ru(III) sites in ligand-bridged dimers like $[(bpy)_2ClRu^{II}(4,4'\text{-bpy})Ru^{III}Cl(bpy)_2]^{3+}$ (bpy = 2,2′-bipyridine). The extent of coupling and the magnitude of $\nu_{et}$ increase with the extent of mixing of the electron-donor and -acceptor wave functions. Using recently derived expressions for $\nu_{et}$ and relating them to the properties of the MMCT or IT bands allows an estimate of $\nu_{et} \approx 10^{13}$ $s^{-1}$ to be made for both the outer-sphere and ligand-bridged complexes.[6,28] Although there could be some unusual feature in the $\nu_{et}$ value for the clusters related to the delocalized nature of the electron-donor and -acceptor orbitals, it seems an unlikely possibility. In the ligand-bridged, mixed-valence cluster dimer, $[(py)_2(CH_3CO_2)_6Ru^I_3O(1,4\text{-pz})Ru^0_3O(CH_3CO_2)_6(py)_2]^+$, evidence exists[9] for a relatively intense IT band ($\epsilon \sim 1000$), showing that appreciable electronic interactions can exist between the clusters, at least through a bridging ligand.

Assuming that $\nu_{et}$ is $10^{12}$–$10^{14}$ $s^{-1}$ gives, from the intercept of the plot in Figure 4, $\Delta S^*_{obsd} + R \ln \nu_{et} = 52$ or $\Delta S^*_{obsd} = \Delta S_A + \Delta S^* = -7 \pm 5$ cal/(mol deg). In comparing the two sets of calculated data in Table V, it seems clear that the more reasonable agreement is obtained by using the statistical approach and eq 28 to calculate $\Delta S_A$. In fact, with the combination of the statistical treatment for $K_A$ and eq 32–34 for the electron-transfer step, reasonably good agreement is obtained between the calculated and experimental kinetic parameters, especially given the innate uncertainty in choosing appropriate values for $d$ and $\nu_{et}$.

However, there is a disconcerting note. At this point, the choice of the Eigen–Fuoss or statistical treatments for the association complex equilibrium is entirely arbitrary. For example, there are cases involving the formation of ion pairs where the Eigen–Fuoss approach works remarkably well.[29] The situation as it stands suggests that it will always be difficult to make detailed comparisons between experiment and theory for outer-sphere reactions not necessarily because of uncertainties in the electron-transfer theory but because of the unavailability of an adequate treatment for association complex formation.

Returning to our attempts to measure the rate of intramolecular electron transfer in the dimer, $[(py)_2(CH_3CO_2)_6Ru^I_3O(1,4\text{-py})Ru^0_3O(CH_3CO_2)_6(py)_2]^+$, it was disappointing that the measurement could not be made, but in retrospect, the failure is not surprising. As a lower limit, the NMR experiment gave $k \geq 7 \times 10^4$ $s^{-1}$ at −70 °C for the inner-sphere electron-transfer rate constant. For the outer-sphere reaction, the rate constant for electron transfer within the association complex (eq 11) can be calculated at −66 °C from the data in Table III by using $K_A = 0.14$ $M^{-1}$ (eq 22) ($\Delta H_A \simeq 0$) and the relation $k_{et} = k/K_A$ (eq 13). The calculated value for $k_{et}$ for the outer-sphere reaction, $k_{et} = 1.4 \times 10^8$ $s^{-1}$, is a factor of 2000 higher than the lower limit set by the NMR study of the dimer.

**Acknowledgments** are made to the Army Research Office—Durham under Grant No. DAAG29-76-G-0135 and to the National Science Foundation under Grant No. CHE77-03423 for support of this research and to Dr. A. K. Gregson for helpful discussions.

**Registry No.** $Ru_3O(CH_3CO_2)_6(py)_3$, 37337-93-2; $[Ru_3O(CH_3CO_2)_6(py)_3]^+$, 51155-94-3; $[(py)_2(CH_3CO_2)_6Ru_3O(1,4\text{-pz})Ru_3O(CH_3CO_2)_6(py)_2]^+$, 70815-83-7; $[(py)_2(CH_3CO_2)_6Ru_3O(1,4\text{-pz})Ru_3O(CH_3CO_2)_6(py)_2]^{2+}$, 55524-12-4; $(py)_2(CH_3CO_2)_6Ru_3O(1,4\text{-pz})Ru_3O(CH_3CO_2)_6(py)_2$, 70812-66-7; $[(py)_2(CH_3CO_2)_6Ru_3O(4,4'\text{-bpy})Ru_3O(CH_3CO_2)_6(py)_2]^{2+}$, 70766-13-1; $[(py)_2(CH_3CO_2)_6Ru_3O(4,4'\text{-bpy})Ru_3O(CH_3CO_2)_6(py)_2]^+$, 70812-67-8; $(py)_2(CH_3CO_2)_6Ru_3O(4,4'\text{-bpy})Ru_3O(CH_3CO_2)_6(py)_2$, 70812-68-9.

**Supplementary Material Available:** Chemical shift and line width data for the acetate protons for solutions containing $[Ru_3O(CH_3CO_2)_6(py)_3]^{+/0}$ in dichloromethane (1 page). Ordering information is given on any current masthead page.

(27) For methylene chloride at 24 °C, $\theta = 1.2°$, from data in: "Handbook of Physics and Chemistry", 48th ed.; CRC Press: Cleveland, OH, 1967.
(28) (a) Curtis, J. C.; Meyer, T. J. *J. Am. Chem. Soc.* **1978**, *100*, 6284. (b) Curtis, J. C.; Sullivan, B. P.; Meyer, T. J. *Inorg. Chem.*, in press.
(29) (a) Prue, J. E. "Ionic Equilibria"; Pergamon: New York, 1966. (b) Gordon, J. E. "The Organic Chemistry of Electrolyte Solutions"; Wiley: New York, 1975.